CDF/PUB/TOP/PUBLIC/9343

Search for Pair Production of Stop Quarks Mimicking Top Event Signatures

The CDF Collaboration
URL http://www-cdf.fnal.gov
May 22, 2008

Abstract

We present the search for the pair-produced super-symmetric partner of the top quark (stop quark) using $1.9 fb^{-1}$ of data collected with CDF II. We search for the scalar top quarks via their decay channel: $\tilde{t}_1 \rightarrow b + \tilde{\chi}_1^{\pm} \rightarrow b + \tilde{\chi}_1^0 + \nu + \ell$ which gives an event signature similar to that of a top dilepton event. We reconstruct events under the stop decay hypothesis and use the reconstructed stop mass as a discriminating kinematic variable in the fit to data. We separate this analysis into two channels, events that contain a b-tagg, and events that do not.

In the signal region the number of events observed and the kinematic distribution of the reconstructed stop mass is consistent with the SM predictions. Thus no evidence for scalar top quark pair-production is observed. We set 95% C.L. limits on the stop production cross section in the three-dimensional space of super-symmetric particle masses, $\tilde{t}_1, \tilde{\chi}_1^{\pm}, \tilde{\chi}_1^0$ assuming 100% branching ratio of stop quark decays into bottom quark and chargino.

1 Introduction

Supersymmetry (SUSY) is one of the most plausible extensions to the Standard Model (SM) of particle physics. It naturally solves the problem with quadratically divergent quantum corrections contributing to the Higgs mass. It predicts unification of gauge coupling constants at a common GUT scale, and provides a natural dark matter candidate. To reconcile the supersymmetry with the experimental data, SUSY must be broken, and the SM particles obtain their superpartners with distinct, mostly much heavier, masses.

However, due to the heaviness of the top quark, the mass splitting between $\tilde{t}_1$ and $\tilde{t}_2$ can be large, such that the lighter top squark $\tilde{t}_1$ is the lightest squark of all, and can be even lighter than the top quark.

The decays of the stop quarks are dictated by the mass spectrum of other supersymmetric particles. For a light stop, $m_{\tilde{t}_1} \lesssim m_t$, and the R-parity conserved SUSY the following decays are possible:

$$\tilde{t}_1 \to c\tilde{\chi}^0_{1,2}, \quad \tilde{t}_1 \to b\,\chi^+_1, \quad \tilde{t}_1 \to W^+\,b\,\tilde{\chi}^0_1, \quad \tilde{t}_1 \to H^+\,b\,\tilde{\chi}^0_1, \quad \tilde{t}_1 \to b\,\tilde{\ell}^+\,\nu_\ell, \quad \tilde{t}_1 \to b\,\tilde{\nu}_\ell\,\ell^+$$

For reasons that will be discussed shortly we choose to investage

$$\tilde{t}_1 \to b\,\chi^+_1 \tag{1}$$

and consider the cases where the $\tilde{\chi}^\pm_1$ can decay to our desired dilepton final state via

$$\tilde{\chi}^\pm_1 \to \tilde{\chi}^0_1 + W^{\pm(*)} \to \tilde{\chi}^0_1 + \ell + \nu \quad (2) \qquad \tilde{\chi}^\pm_1 \to \tilde{\chi}^0_1 + H^{\pm *} \to \tilde{\chi}^0_1 + \ell + \nu \quad (3)$$

$$\tilde{\chi}^\pm_1 \to \ell + \tilde{\nu}_\ell \to \tilde{\chi}^0_1 + \ell + \nu \quad (4) \qquad \tilde{\chi}^\pm_1 \to \nu + \tilde{\ell}_L \to \tilde{\chi}^0_1 + \ell + \nu \quad (5)$$

$$\tilde{\chi}^\pm_1 \to \tilde{\chi}^0_1 + G^{\pm *} \to \tilde{\chi}^0_1 + \ell + \nu \quad (6)$$

Where if $m_{\tilde{\chi}^\pm_1} - m_{\tilde{\chi}^0_1} \geq m_{W^\pm}$ then (2) will dominate over the other possible decay means. If the charginos decay through (2), then the dilepton branching ratio of stop events will be the same as top events, 0.11. However, when the other chargino decay modes are possible, the dilepton branching ratios will become dependent on other SUSY parameters, and can possible greatly enhance the dilepton branching ratio. For instance, the MC we generated at $m_{\tilde{\chi}^\pm_1} = 105.8$ and $m_{\tilde{\chi}^0_1} = 58.8$ GeV has a dilepton branching ratio of 0.25 at $tan\beta = 5$, but at $tan\beta = 15$ the dilepton branching ratio increases to 0.50.

1.1 Motivations for this Search

In this analysis we explore a possibility that $m_{\tilde{t}_1} \lesssim m_t$, as demanded by some supersymmetric electroweak baryogenesis scenarios [1], and that the LSP is the neutralino (χ^0_1), as favored by the astrophysical data [3], and the chargino is lighter than the stop quark. We also assume $m_{\tilde{\chi}^\pm} < m_{\tilde{t}_1} - m_b$, in which case the channel (1) opens and

becomes dominant with almost 100% branching ratio. Although in this scenario the mass splitting between stop and neutralino is large, the agreement with WMAP data can still be satisfied [4].

The channel (1) with the subsequent decays (2) through (5) is interesting independently of aforementioned theoretical arguments, since although this possibility has been studied at both CDF and D0 [10, 5], no experimental limits on masses of supersymmetric particles have been set, and it still remains "*terra incognita*".

Another motivation for this search is that in the decay scenario we investigate the scalar tops decay products are identical to those from the decays of top quarks, but with two neutralinos in the final state. Therefore if Nature allows this possibility, stop events would enter the top quark data sample and mimic the top event signatures, thus affecting top properties measurements.

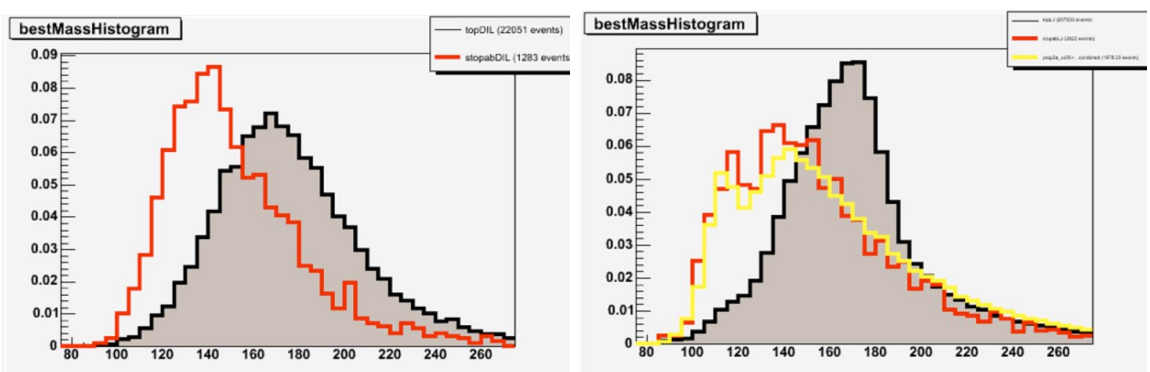

Figure 1: Results of the top mass fitter ran over events with $m_{\tilde{t}} = 155$, $m_{\tilde{\chi}_1^+} = 105.8$, and $m_{\tilde{\chi}_1^0} = 58.8$ monte carlo sample for dilepton events (left) and lepton + jets events (right). Filled histogram is $t\bar{t}$, red histogram is stop and yellow histogram is W + jets, the major background for $t\bar{t}$ in lepton + jets channel.

As one can conclude from 1 that given the top quark sample had an admixture of stop events, the measured top mass in the dilepton channel would be biased towards lower value, while the measurement would not be affected in the lepton + jets channel due to stop mimicking the much larger background of W + jets. This discrepancy of measured top mass between the channels is exactly the tendency that was present in the CDF and D0 measurements in the dilepton and lepton + jets channels in Run I and early Run II data.

This observation served as a motivation for the current analysis. Although recent measurements in the dilepton channel are more consistent with those in lepton + jets, such as [7], the analysis also use looser event selection, while the cross sections in the tight tagged top dilepton channel are still being measured higher than predicted in the SM, with slightly discrepant kinematics [11, 12], giving plenty of room for new physics.

1.2 Stop Quark Production at the Tevatron

At the Tevatron the stop quarks would be produced in pairs via the QCD processes shown in in Figure 2. The stop quark pair production cross section depends on the stop quark mass, and it is independent on other SUSY parameters. The NLO production cross sections for various stop masses are listed in Table 3. They were obtained using PROSPINO 2.0 [**?**] and CTEQ6M (NLO) parton distribution functions.

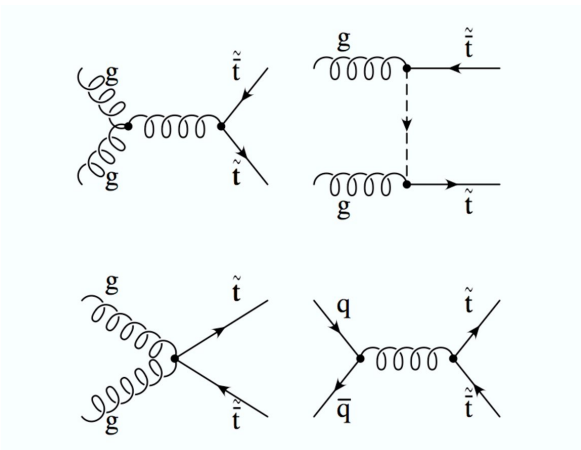

Figure 2: The dominant processes for stop quark pair production at the Tevatron.

$m_{\tilde{t}_1}$, GeV	Cross Section (pb)
115.0	6.89
135.0	2.77
155.0	1.23
185.0	0.416

Figure 3: Cross section in pb for $\tilde{t}\bar{\tilde{t}}$ production at the Tevatron.

2 Methodology

2.1 Goals

What distinguishes this search from most other SUSY searches is that one can obtain results independent of the complex multi-dimensional phase space of SUSY parameters. The minimal assumptions made here are:

1. $\tilde{\chi}_1^0$ is the LSP, and $\tilde{q}, \tilde{\ell}, \tilde{\nu}$ are heavy
2. $m_{\tilde{t}_1} \lesssim m_t$
3. $m_{\tilde{\chi}_1^+} < m_{\tilde{t}_1} - m_b$

If these requirements are satisfied then channel (1) has a 100% branching ratio. The rate with which the $\tilde{t}_1\bar{\tilde{t}}_1$ events are produced depend on $m_{\tilde{t}_1}$, and kinematics of the stop events depend on masses of supersymmetric particles: $(m_{\tilde{t}_1}, m_{\tilde{\chi}_1^+}, m_{\chi_1^0})$

Therefore in this analysis we aim to explore the three-dimensional phase space of masses of these super-symmetric particles, and in the absence of new physics evidence we can derive limits on masses of $\tilde{t}_1, \tilde{\chi}_1^{\pm}, \tilde{\chi}_1^0$ independent on other SUSY assumptions.

3 Data Sample and Dilepton Selection

Typically high energy physics analyses start with finalizing an event selection for the search, and then proceed to estimate contributions from backgrounds in the signal region, as well as derive systematic uncertainties, and verify background modeling in the control regions. For this search we saved finalizing event selection until nearly the last step, so as to optimize the event selection, taking into account nearly all of our systematic uncertainties. We first verified that in all of our dilepton control regions, where we expected little or no signal, that we could adequately model both the rate and relevant kinematics of the backgrounds. We then created prescriptions for computing all of our systematics, so as to use the highly discriminating reconstructed stop mass variable and chose our final event selection cuts based on nearly all systematics, optimizing on expected exclusion.

3.1 Event Selection

We require 2 leptons (e or μ) with $P_T > 20$ GeV, requiring at least one of the leptons to be isolated from calorimeter energies not associated with that lepton, one of the leptons must also trigger the event. If the leptons in the event are either both electrons or both muons, and form an invariant mass near the Z-pole mass, we apply an additional Z-veto that requires Met Significance $\equiv \frac{\not{E}_T}{\sqrt{\sum E_T}} > 4$ GeV, Since stop event contain undetected particles, we require events to have ≥ 20 GeV of missing transverse energy. For b-tagged events we require the leading jet to have at least 15 GeV of transverse energy, and the second jet to have at least 12 GeV. For the non-tagged events, we require the leading two jets to both have at least 20 GeV of transverse energy.

To help remove the remaining dominant standard model background, $t\bar{t}$, we make a cut in the $H_T \equiv \sum_{allobj.} P_T$ v. $\Delta\phi\,(jets) \times \Delta\phi\,(leptons)$ plane. As can be seen from Figure 4 requiring events to pass

$$H_T < 215 + \frac{\Delta\phi\,(jet_0, jet_1)\,\Delta\phi\,(lep_0, lep_1)}{\pi^2} \times 325 \tag{7}$$

substantially reduces the number of top events by a factor of 2 while reducing stop by approximately only 12%.

4 Data Sample and Physics Modeling

This analysis is based on the data collected by CDF II between March 2002 and March 2007 using inclusive high-P_T lepton triggers. To model backgrounds we use both monte carlo and data derived backgrounds. For the stop signal simulation we use PYTHIA, with input we specify the stop mass, U(1) and SU(2) gaugino parameters (M_1 and M_2). The values M_1 and M_2 are approximately equal to neutralino ($\tilde{\chi}_1^0$) and chargino ($\tilde{\chi}_1^+$) masses. We also set the stop mixing angle to unity, and $\tan\beta = 5.0$. Note that the

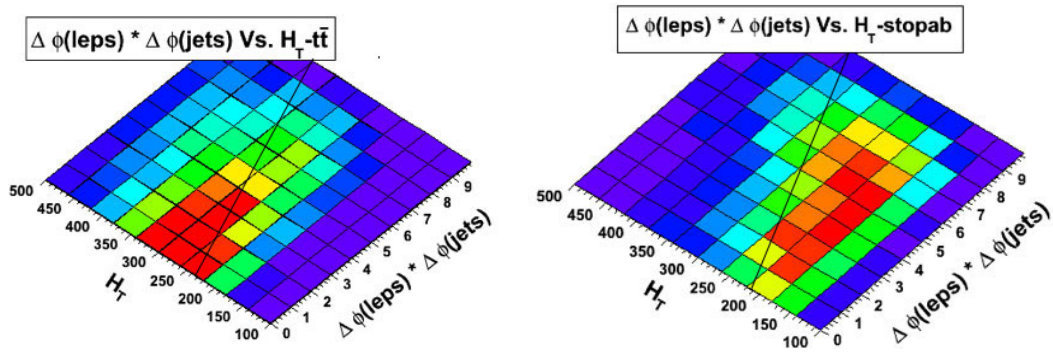

Figure 4: The H_T verses $\Delta\phi\,(leptons)\,\Delta\phi\,(jets)$ for top events (left), and stop events (right). It can been seen that stop events tend to lie at a lower H_T and larger $\Delta\phi_{\ell\ell}\Delta\phi_{jj}$. Making a diagonal cut in this plane efficiently removes top events, while keeping stops. The lines drawn correspond to $H_T = 215 + \frac{\Delta\phi(jet_0,jet_1)\Delta\phi(lep_0,lep_1)}{\pi^2} \times 325$

actual values of these two parameters are irrelevant, since they define mixing between light and heavy stop quarks, and in the case that $m_{\tilde{\chi}_1^\pm} - m_{\tilde{\chi}_1^0} \geq m_{W^\pm}$ how much each of the decays (2) through (5) contribute. We have found the kinematics of the events does not largely depend on which channel chargino decays through. Also the cross section of pair produced stop quarks does not depend on the mixing, but on the actual value of the stop mass only. Similarly, the actual relationships between $m_{\tilde{\chi}_1^+}$ and M_2, and between $m_{\tilde{\chi}_1^0}$ and M_1 are irrelevant, since masses of the supersymmetric particles will determine the acceptance and kinematics of the stop events.

We have generated various stop MC samples in the SUSY mass ranges

$$115 \leq m_{\tilde{t}_1} \geq 185 \tag{8}$$

$$105.8 \leq m_{\tilde{\chi}_1^\pm} \geq 125.8 \tag{9}$$

$$43.9 \leq m_{\tilde{\chi}_1^0} \geq 88.5 \tag{10}$$

We are then able to interpolate between our generated samples through a template morphing technique, for both signal and background templates. This allows us to obtain any combination of $m_{\tilde{\chi}_1^\pm}$, $m_{\tilde{\chi}_1^0}$, and $m_{\tilde{\chi}_1^\pm}$, that is within the signal MC we have generated. We have verified this morphing procedure through generating additional signal MC samples and verifying that the results of morphing templates accurately reproduces the reconstructed stop mass templates of the additional stop samples.

4.1 Standard Model Backgrounds

To model the dominant background to this search, $t\bar{t}$, we use PYTHIA monte carlo, taking the top mass to be 172.5 GeV with an uncertainty of 1.5 GeV. This is approximately the current world average top mass and uncertainty [8]. We use the NLO cross section at a given top mass to normalize the top contribution. In treating the uncertainty due to the in precisely known top mass, we take into account the rate difference to to both cross-section and acceptance, as well as the shape difference caused by changing the top mass.

We make use of inclusive diboson samples generated with PYTHIA and $W\gamma$ samples generated with Baur. We use the respective NLO cross sections to normalize these physics processes.

For $Z/\gamma^\star + jets$ process modeling we use the Matrix Element ALPGEN $Z/\gamma^\star \rightarrow \ell^+\ell^-$, $(\ell = e, \mu, \tau)$ events produced in association with light and heavy flavor jets and PYTHIA for parton shower simulation. Since ALPGEN is a leading order monte carlo generator we normalize $Z/\gamma^\star$ cross section to data in the control region of low $\not\!\!E_T$, and $76 < m_{\ell\ell} < 106$ GeV. We use the normalization difference between found in this region to normalize our $Z/\gamma^\star$ events outside of the $76 < m_{\ell\ell} < 106$ GeV region, separately for the tagged and anti-tagged channels. As the uncertainty on this normalization we use the statistical uncertainty plus the difference in normalization in ee v $\mu\mu$ events, although it should be noted that predictions for ee v $\mu\mu$ events are consistent within statistical errors.

To model events where an identified lepton was actually fake, e.g. events from $t\bar{t} \rightarrow \ell$ + jets, W+jets and QCD processes, we use a large sample of generic jets to parameterize the probability that a jet will pass all electron or muon identification requirements. We apply these parametrized probabilities to lepton plus electron or muon like events to find the contribution of fake events in our signal region. To parametrize the probability of a jet faking a lepton we use events from a jet sample with a trigger jet of $E_T > 50$ GeV, and parameterize by fake lepton p_T as well as type of lepton, and where in the detector the fake lepton occurred. We use jet samples triggered by 20 GeV, 70 GeV, and 100 GeV E_T jets to derive our uncertainties for this background.

We take into account the differences in lepton identifications between MC and data via use of scale factors derived from comparing unbiased data to MC. Similarly to account for various event trigger and reconstruction efficiencies we use scale factors as well. To account for the different efficiencies in b-tagging between MC and data we a combination of scale factors and parameterized mistagg probabilities. We also take into account all uncertainties on the scale factors.

To account for uncertainties in the measured jet energies, we shift energies of jets corresponding to MC derived backgrounds and signal up and down by $\pm 2\sigma$ of their jet energy resolutions, and re-run the stop mass reconstruction and event selection algorithms, taking both rate and shape uncertainties into account in setting the limits. Additionally for the $Z/\gamma^\star + jets$ background we use constraints to the data in our control region to help minimize the impact of this uncertainty.

To account for the uncertainty of initial state and final state radiation we have generated MC samples for both top and stop, with increased and decreased amounts of initial/final state radiation as compared to nominal. Moreover, since we cannot tell the difference between initial and final state radiation, we either simultaneously increase both the initial and the final state radiation, or we decrease both.

For signal and non-data derived, or non-data constrained backgrounds we take a 5.9% uncertainty on integrated luminosity. For signal and monte carlo based backgrounds we also take into account theoretical cross section uncertainties.

5 Stop Mass Reconstruction

Given our desire to set smooth confidence limits in SUSY mass space, rather than just setting limits for discreet points corresponding to the MC we generated, we need a single discriminating variable, thus we cannot use a Neural Network, or some other multivariate tequnique that is highly dependent on event kinematics, since these vary depending on SUSY masses. Full reconstruction of the stop events is used to obtain a single highly-discriminating variable between stop events corresponding to various SUSY mass points and the Standard Model backgrounds.

Dilepton stop decays produce four observable particles in the final state plus the missing energy due to additional four undetected neutrinos and neutralinos. This leads to a severely under-constrained system of particle four-momenta equations, making event reconstruction very challenging. However, through the use of a few approximations and assumptions on the $\tilde{\chi}_1^{\pm}$ masses as described below, we can do quite a decent job of reconstructing the original stop quarks kinematics and mass.

5.1 Pseudo-Particle Approximation

One of the most important approximation we make is combining four-momenta of $\tilde{\chi}_1^0$ and ν coming from each $\tilde{t}_1$ together and treat them as one massive Pseudo-Particle, as can be justified from 5.

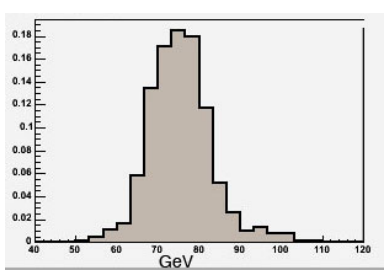

Figure 5: The invariant mass of the Pseudo-Particle ($\tilde{\chi}_1^0 + \nu$) at the generator level, corresponding to $\tilde{t}_1$ mass of 135 GeV, $\tilde{\chi}_1^{\pm}$ mass of 110 GeV, $\tilde{\chi}_1^0$ mass of 60 GeV.

5.2 Jet-To-Parton Assignment

To successfully reconstruct the stop mass we must accurately assign the $b(\bar{b})$ and the proper lepton. We use logic based on jet-lepton invariant mass quantities and successfully pair the correct jet-to-lepton 85% to 95% of the time, when both b-jets are in the leading two jets of the event.

5.3 Weighting Method

After making the Pseudo-Particle approximation and placing the $\tilde{\chi}_1^{\pm}$ - mass constraint, the event kinematics is still underconstrained (a -1C system), such that it is not possible to reconstruct kinematics of the event uniquely. We develop the method similar to the top dilepton neutrino weighting technique [6]. For a given Pseudo-Particle's ϕ direction combination we minimize a χ^2 function 11 via TMinuit, and then perform a weighted sum over all ϕ combinations to create the reconstructed kinematics of the event.

5.4 The χ^2 Minimization Process

We construct the χ^2 function as follows

$$\begin{aligned}\chi^2 = & \frac{\left(\vec{\ell}_{meas} - \vec{\ell}_{fit}\right)^2}{\sigma_\ell^2} + \frac{\left(\vec{\bar{\ell}}_{meas} - \vec{\bar{\ell}}_{fit}\right)^2}{\sigma_\ell^2} + \frac{\left(\vec{u}_{meas} - \vec{u}_{fit}\right)^2}{\sigma_{uncl}^2} \\ & + \sum_{jets\, i} \frac{\left(\vec{j}_{i_{meas}} - \vec{j}_{i_{fit}}\right)}{\sigma_{jet_i}^2} + \frac{\left(M_{PP_1}^{fit} - M_{PP}^{assume}\right)^2}{\Gamma_{PP}^{gen}} \\ & + \frac{\left(M_{PP_2}^{fit} - M_{PP}^{assume}\right)^2}{\Gamma_{PP}^{gen}} + \frac{\left(M_{PP_1,\ell} - M_{\tilde{\chi}^\pm}\right)^2}{\Gamma^{\tilde{\chi}^\pm}} \\ & + \frac{\left(M_{PP_1,\bar{\ell}} - M_{\tilde{\chi}^\pm}\right)^2}{\Gamma^{\tilde{\chi}^\pm}} + \frac{\left(M_{PP_1,\bar{\ell},b_{jet}} - M_{PP_2,l,\bar{b}_{jet}}\right)}{\Gamma^{\tilde{t}}}\end{aligned} \tag{11}$$

where $\vec{\ell}_{meas}$ is the lepton measured momentum and $\vec{\ell}_{fit}$ is the fitted lepton momentum. Similarly u refers to the unclustered energy in the event, which includes all jets except for the assumed b-jets that originate from the stop decay. PP_i are Pseudo-Particles. The first four terms in the χ^2 function refer to how the measured physics quantities are allowed to vary within their estimated uncertainties.

We consider each ϕ-combination of Pseudo-Particles directions, and construct a sum of reconstructed stop masses for all possible combinations that are weighted according to χ^2 of the fit to yield the reconstructed stop mass of an event:

$$M_{\tilde{t}_1}^{Reco} = \frac{1}{\sum_{\phi\, i,j} e^{-\chi_{i,j}^2}} \sum_{\phi\, i,j} M_{i,j}^{fit} e^{-\chi_{i,j}^2} \tag{12}$$

Events per 1.9 fb^{-1} in the anti-tag signal region

Source	ee	$\mu\mu$	$e\mu$	$\ell\ell$
stop(155,105,60)	0.77 ± 0.16	0.91 ± 0.19	2.18 ± 0.44	3.87 ± 0.79
top	4.63 ± 0.69	4.69 ± 0.71	10.31 ± 1.52	19.63 ± 2.73
Z + HF Jets	0.24 ± 0.04	0.22 ± 0.04	0.07 ± 0.01	0.52 ± 0.10
Z + LF Jets	8.85 ± 0.49	6.55 ± 0.36	2.99 ± 0.17	18.39 ± 1.02
diboson	1.30 ± 0.16	1.04 ± 0.13	2.44 ± 0.31	4.78 ± 0.60
fakeables	2.03 ± 0.61	1.09 ± 0.33	3.88 ± 1.16	7.00 ± 2.10
SM Total	17.06 ± 1.53	13.58 ± 1.17	19.69 ± 2.75	50.32 ± 5.41
Data	23	5	20	48

Table 1: Predicted v. observed number of events in the in signal untagged region. For comparison the expectations a SUSY mass points is given.

5.5 Likelihood Fitter

We employ the CL_s limit-setting technique [9] that is based on the likelihood ratio test statistics:

$$Q = \frac{L(\text{data} \mid \text{signal + background})}{L(\text{data} \mid \text{background only})} \tag{13}$$

The likelihood ratio fit on the combination of the reconstructed stop mass templates is performed using TMinuit. The systematic uncertainties enter the fit as Gaussian constraint nuisance parameters. We allow the signal and background predictions float within their rate uncertainties, and allow the mass template shape variations using the Morphing Technique.

6 Results

The expected numbers of events from various SM backgrounds are given in Tables 1 and 2 for the anti-tag and the tag region respectively. Shown in 6 through 6.2 is the cross section excluded as a function of stop mass, for fixed $\tilde{\chi}_1^{\pm}$ and $\tilde{\chi}_1^0$ masses. It should be noted that these limits assume a dilepton branching ratio of 0.11.

6.1 Accepted Number of Events

6.2 Limits And Data Comparisons

Below is shown the cross section we exclude at the 95% CL assuming the dilepton branching ratio of 0.11, that is that $m_{\tilde{\chi}_1^{\pm}}$ decays via a SM W boson. As stated in section 2, if $m_{\tilde{\chi}_1^{\pm}} - m_{\tilde{\chi}_1^0} \geq m_{W^{\pm}}$ then addition chargino decay modes will become open, and the dilepton branching ratio can be greatly enhanced. Also shown is

Events per 1.9 fb^{-1} in the signal region with ≥ 1 tag.

Source	ee	$\mu\mu$	$e\mu$	$\ell\ell$
stop(155,105,60)	0.29 ± 0.06	0.34 ± 0.06	0.83 ± 0.16	1.46 ± 0.28
top	4.38 ± 0.64	4.45 ± 0.66	9.85 ± 1.36	18.68 ± 2.46
Z + HF Jets	0.26 ± 0.05	0.20 ± 0.04	0.07 ± 0.01	0.54 ± 0.10
Z + LF Jets	9.33 ± 2.57	6.77 ± 2.10	3.13 ± 0.25	19.23 ± 4.91
Diboson	1.40 ± 0.25	1.05 ± 0.21	2.46 ± 0.45	4.91 ± 0.91
Fakes	1.65 ± 0.49	1.98 ± 0.59	5.02 ± 1.51	8.66 ± 2.60
Total	17.02 ± 3.01	14.46 ± 2.59	20.54 ± 3.28	52.02 ± 8.04
Data	20	6	20	46

Table 2: Predicted v. observed number of events in the in signal tagged region. For comparison the expectations from a SUSY mass points is given.

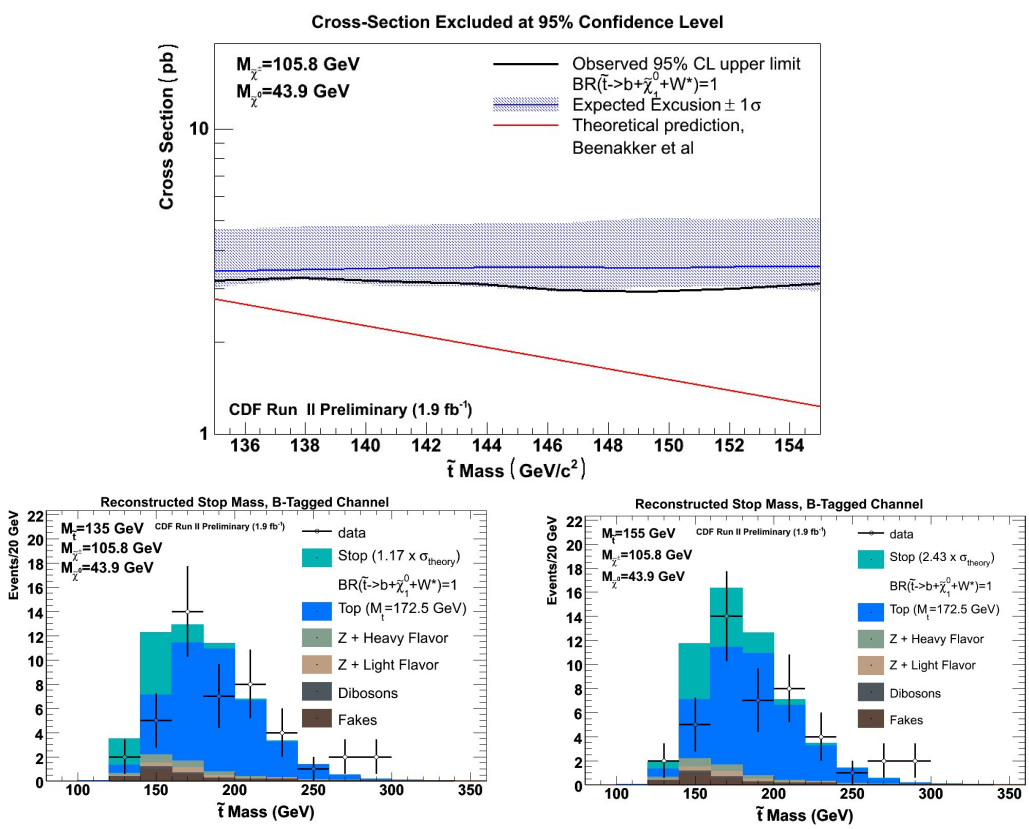

Figure 6: Cross section excluded at 95% CL, for $m_{\tilde{\chi}_1^\pm} = 105.8$ GeV and $m_{\tilde{\chi}_1^0} = 43.9$ GeV, and some representive reconstructed stop mass templates plotted at their excluded cross sections

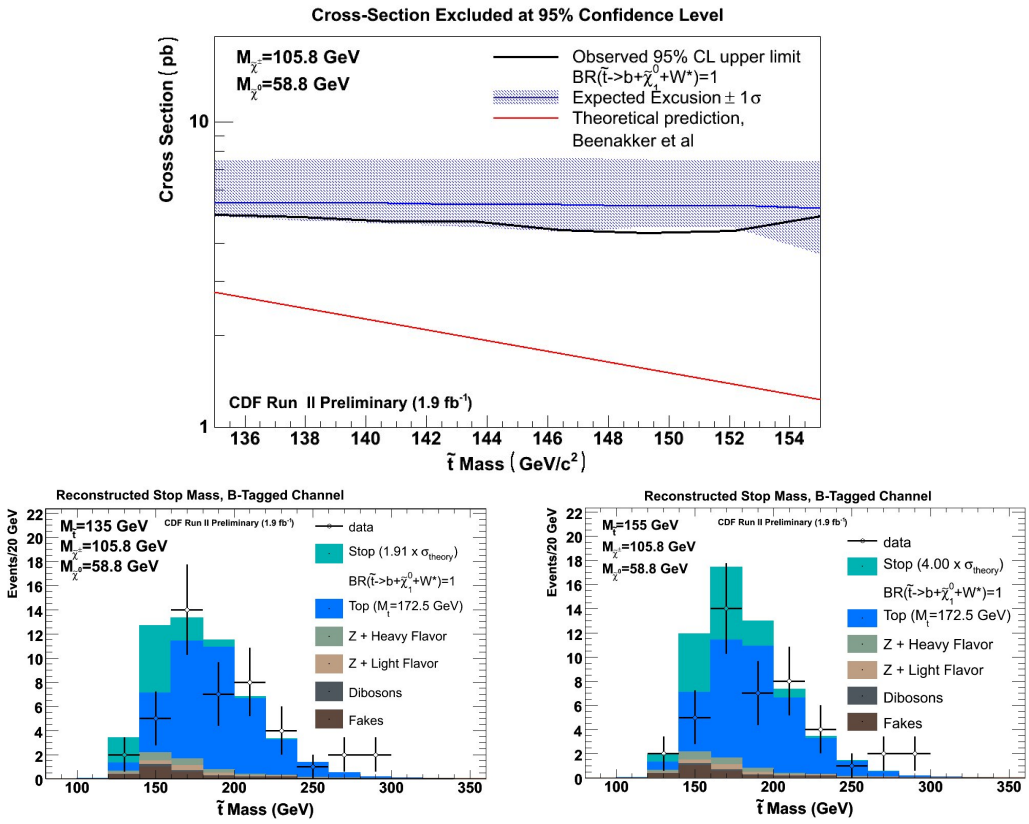

Figure 7: Cross section excluded at 95% CL, for $m_{\tilde{\chi}_1^{\pm}} = 105.8$ GeV and $m_{\tilde{\chi}_1^0} = 58.8$ GeV, and some representive reconstructed stop mass templates plotted at their excluded cross sections

References

[1] C. Balazs, M. Carena and C. Wagner, Phys. Rev. **D** 70 (2004) 015007, [arXiv:hep-ph/0403224v2].

[2] T. Aaltonen *et al.*, The CDF Collaboration, Phys. Rev. **D**76, 072010 (2007), [arXiv:0707.2567].

[3] W. M. Yao *et al.* [Particle Data Group], J. Phys. G **33**, 1 (2006).

[4] S. Abdullin *et al.*, FERMILAB-CONF-06-284-T, [arXiv:hep-ph/0608322v2].

[5] S.-J. Park, the D0 Collaboration, [arXiv:hep-ph/0710.1016v1].

[6] G. Bellettini *et al.*, CDF Note 9048.

[7] B. Jayatilaka *et al.*. CDF Note 9130.

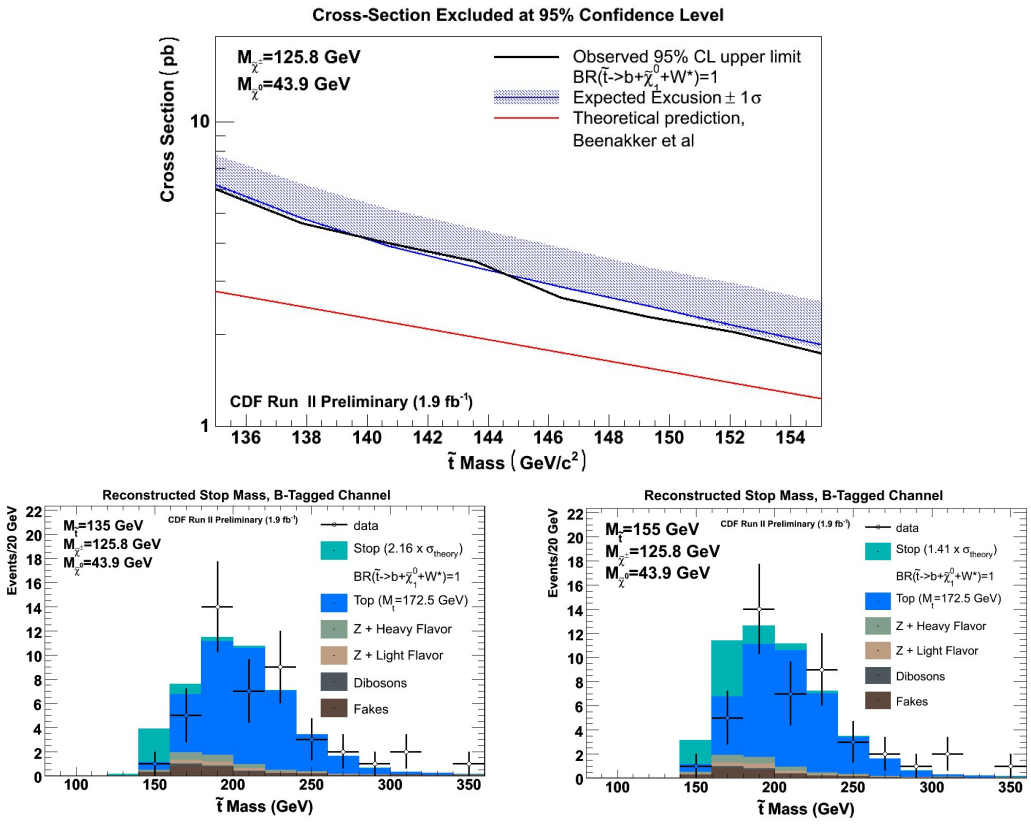

Figure 8: Cross section excluded at 95% CL, for $m_{\tilde{\chi}_1^\pm} = 125.8$ GeV and $m_{\tilde{\chi}_1^0} = 43.9$ GeV, and some representive reconstructed stop mass templates plotted at their excluded cross sections

[8] D. Glenzinski *et al.*, [arXiv:hep-ex/0603039v1]

[9] T. Junk, CDF Note 8128.

[10] T. Affolder *et al.*, The CDF Collaboration, Phys. Rev. Lett. 84, 5273 (2000), (CDF Note 5099)

[11] A. Varganov *et al.*, CDF Note 9210.

[12] T. Spreitzer *et al.*, CDF Note 8696.

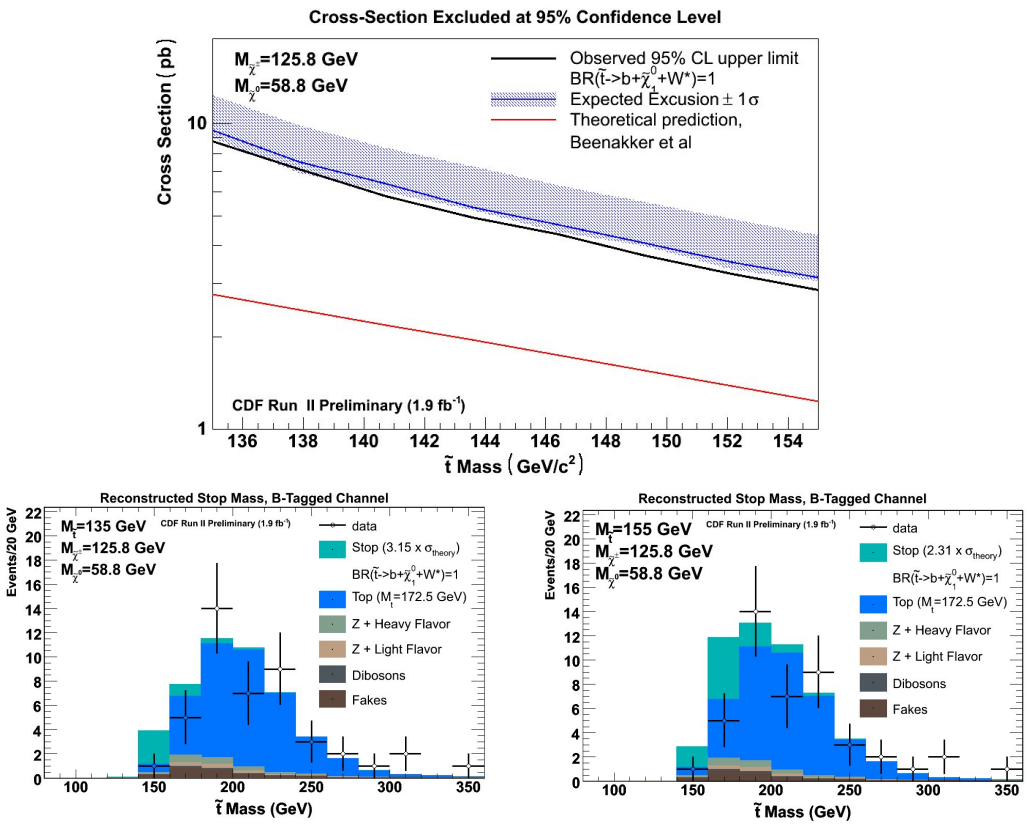

Figure 9: Cross section excluded at 95% CL, for $m_{\tilde{\chi}_1^\pm} = 125.8$ GeV and $m_{\tilde{\chi}_1^0} = 58.8$ GeV, and some representive reconstructed stop mass templates plotted at their excluded cross sections